Molecular structure determination from x-ray scattering patterns of laser-aligned symmetric-top molecules

P. J. Ho,[1] D. Starodub,[2] D. K. Saldin,[3] V. L. Shneerson,[3] A. Ourmazd,[3] and R. Santra[1,4,a)]
[1]*Argonne National Laboratory, Argonne, Illinois 60439, USA*
[2]*Department of Physics, Arizona State University, Tempe, Arizona 85287, USA*
[3]*Department of Physics, University of Wisconsin-Milwaukee, Milwaukee, Wisconsin 53201, USA*
[4]*Department of Physics, University of Chicago, Chicago, Illinois 60637, USA*

(Received 14 July 2009; accepted 19 September 2009; published online 5 October 2009)

We investigate the molecular structure information contained in the x-ray diffraction patterns of an ensemble of rigid CF_3Br molecules aligned by an intense laser pulse at finite rotational temperature. The diffraction patterns are calculated at an x-ray photon energy of 20 keV to probe molecular structure at angstrom-scale resolution. We find that a structural reconstruction algorithm based on iterative phase retrieval fails to extract a reliable structure. However, the high atomic number of Br compared with C or F allows each diffraction pattern to be treated as a hologram. Using this approach, the azimuthal projection of the molecular electron density about the alignment axis may be retrieved. © *2009 American Institute of Physics*. [doi:10.1063/1.3245404]

Currently available short, intense laser pulses can strongly perturb molecules, leading to molecular alignment, deformation, ionization, and/or fragmentation.[1] Particularly exciting is the prospect to impose new, time-dependent molecular structures during the laser pulse.[2,3] Molecules in strong laser fields have been studied by employing ion imaging techniques.[4–9] These approaches, though powerful, are restricted to small molecules and do not provide detailed information on the molecular structure in the laser field. A promising alternative technique is ultrafast x-ray scattering,[10,11] which may potentially be used to directly probe the laser-induced structure of molecules of arbitrary size with subnanometer resolution.

An ensemble of molecules of interest in the gas or liquid phase can serve as a sample in x-ray scattering studies, provided that a high degree of spatial alignment is achieved.[12–15] The far-field scattering pattern obtained over many x-ray pulses is then an incoherent sum of scattering patterns from individual molecules, thus reflecting the signal of a single molecule with an enhancement factor proportional to the number of molecules.[12–14] The interaction potential between an intense laser field and a molecule depends on the Euler angles connecting the principal axes of the molecular polarizability tensor with the laboratory frame defined by the laser field. This forms the basis of a powerful, general technique for aligning molecules.[16] Highly aligned molecular ensembles are readily available in the laser intensity regime where laser-induced structures occur, suggesting that ultrafast x-ray scattering from laser-aligned molecules might be an ideal tool to study the structure of laser-dressed molecules. Here, we address the capabilities and limitations of this potentially important approach.

With an intense, elliptically polarized laser pulse, three-dimensional (3D) alignment of asymmetric-rotor molecules can be achieved.[17–19] It is not necessary to control the orientation of the molecules,[20–23] since the molecular structure can be uniquely determined from diffraction patterns of a spatially aligned sample.[24] Unlike asymmetric-rotor molecules, the rotational dynamics of symmetric-top molecules about their symmetry axis cannot be restricted with elliptically polarized light (unless the molecules undergo a laser-induced distortion and become asymmetric rotors). In other words, 3D alignment of symmetric-top molecules in a laser field is not possible. As a result, the x-ray diffraction patterns of laser-aligned symmetric-top molecules are necessarily averaged with respect to rotations about the molecular symmetry axis.

This raises the question whether it is possible to retrieve useful molecular structure information in the presence of this unavoidable rotational averaging. By analyzing simulated diffraction patterns of the symmetric-top molecule bromotrifluoromethane (CF_3Br) as a representative example, we investigated the extent to which different structure reconstruction methods can yield reliable information from rotationally averaged diffraction patterns. We focused on structure reconstruction methods that are applicable not only to small molecules such as CF_3Br, but also to complex molecules such as proteins. CF_3Br was selected because its alignment dynamics in a strong laser field have been studied experimentally using resonant x-ray absorption.[15] Our findings can be summarized as follows. (1) It is difficult to obtain reliable structural information by iterative phasing techniques.[25] (2) Exploiting the presence of the heavy Br atom, reconstruction of the molecular geometry of CF_3Br is successful. (3) The resolution of the reconstructed molecular structure is not limited by the maximum x-ray momentum transfer recorded, but by the imperfect molecular alignment in the laser field.

We calculated the x-ray scattering patterns of laser-aligned CF_3Br molecules using the methods and molecular parameters described in Refs. 26 and 27. The initial rotational temperature was set to 1 K to mimic the best realisti-

a)Electronic mail: rsantra@anl.gov.

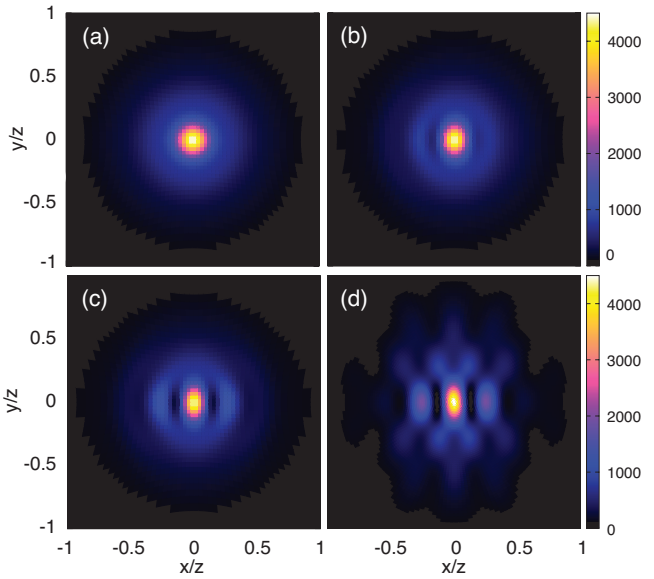

FIG. 1. X-ray diffraction patterns of CF_3Br molecules at 1 K subjected to a 95 ps laser pulse and a 120 ps x-ray pulse for different laser geometries. (a) $\theta_{dl}=0$, (b) $\theta_{dl}=\pi/4$, and (c) $\theta_{dl}=\pi/2$. Here, θ_{dl} is the angle between the x-ray propagation axis and the laser polarization vector. The laser polarization vector lies on a plane defined by the x-ray propagation and polarization vectors. Panel (d) is obtained with the same laser geometry as in (c), except perfect 1D alignment is assumed.

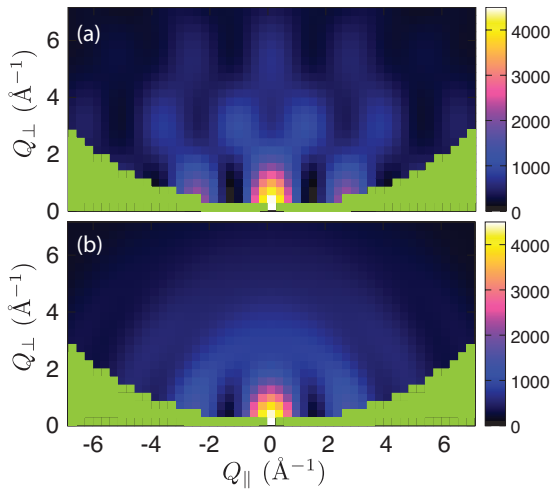

FIG. 2. X-ray diffraction patterns plotted in the two-dimensional subspace of reciprocal space described in the text. The data in panel (a) correspond to Fig. 1(d); (b) corresponds to Fig. 1(c). The green regions indicate the missing wedges.

cally achievable experimental situation.[28] We assumed a linearly polarized 95 ps laser pulse with a peak intensity of 1.9×10^{12} W/cm^2, resulting in quasiadiabatic alignment with a maximum $\langle\cos^2\theta_{ml}\rangle$ of 0.87, where θ_{ml} is the angle between the molecular symmetry axis and the laser polarization axis. This laser-aligned sample was then probed by a 120 ps, 20 keV x-ray pulse. The time delay between the laser and x-ray pulses was set to zero. The gas target was placed at the origin of the laboratory frame. The x-ray scattering patterns were calculated on a detector plane parallel to the *x*-*y* plane of the laboratory frame. The detector plane was located at a distance z from the target, the z axis coinciding with the propagation axis of the incoming x rays. The laser and x-ray parameters used are similar to those employed in the x-ray absorption experiment discussed in Ref. 15.

Our calculated x-ray scattering patterns in the detector plane are shown in Fig. 1. Each pattern is the result of incoherent averaging due to the unrestricted rotational motion about the molecular symmetry axis. In panels (a), (b), and (c) of Fig. 1, there is additional incoherent averaging as a consequence of the imperfect alignment of the molecular symmetry axis by the laser pulse. Effectively, this reduces the achievable resolution. A comparison of panels (c) and (d) demonstrates that imperfect laser-induced alignment causes the x-ray scattering pattern at high scattering angles to be washed out. Nevertheless, the patterns in panels (a), (b), and (c) clearly reflect the fact that, by rotating the polarization axis of the laser, the alignment of the molecular ensemble with respect to the x-ray detector can be controlled.

As a consequence of the rotational averaging, the x-ray scattering pattern in reciprocal space is cylindrically symmetric with respect to the laser polarization axis. Therefore, after introducing cylindrical coordinates in reciprocal space, with the laser polarization axis as the cylinder axis, the scattering intensity depends only on two coordinates in reciprocal space: The coordinate $Q_\parallel$ along the laser polarization axis and the coordinate $Q_\perp$ perpendicular to the laser polarization axis. In the case of perfect one-dimensional (1D) alignment, the molecular symmetry axis coincides with the laser polarization axis.

The accessible area in the $Q_\parallel$-$Q_\perp$ plane depends on the x-ray wavelength, the lab-frame angular coverage provided by the detector, and the angle θ_{dl} between the laser polarization axis and the x-ray propagation axis. A maximum scattering angle of $\theta_{\max}$ with respect to the x-ray propagation axis implies that

$$Q_\parallel^2+Q_\perp^2\leq\frac{16\pi^2}{\lambda^2}\sin^2(\theta_{\max}/2), \tag{1}$$

where λ is the x-ray wavelength. Thus, for a given $\theta_{\max}$, the accessible $Q_\parallel$-$Q_\perp$ region forms a semicircle.

A scattering pattern obtained for a single θ_{dl} does not provide full coverage of this semicircle. In fact, each pattern in panels (a), (b), and (c) of Fig. 1, when restricted to a circular region centered at $x=y=0$, covers a different subset of the accessible semicircle in the $Q_\parallel$-$Q_\perp$ plane. In the $\theta_{dl}=0$ configuration, only scattering intensities along the line $Q_\perp=|Q_\parallel|\sqrt{4\pi/(\lambda|Q_\parallel|)-1}$ are accessible. Away from this configuration, the area covered in the $Q_\parallel$-$Q_\perp$ plane grows. Maximum coverage is obtained when $\theta_{dl}=\pi/2$.

In Fig. 2, we plot x-ray scattering intensities in the $Q_\parallel$-$Q_\perp$ plane for $\theta_{dl}=\pi/2$. In the regions shown in green, the so-called *missing wedges*,[29] scattering intensities are not available as a consequence of the incomplete $Q_\parallel$-$Q_\perp$ coverage for a single θ_{dl}. Interestingly, Saldin *et al.*[25] recently found that, in spite of the missing wedges, the diffraction data from just the $\theta_{dl}=\pi/2$ configuration can be sufficient for reconstruction. The inherent redundancy in oversampled diffraction data[11] appears to overcome the lack of diffraction information in the missing wedges.

In the following, we discuss two approaches to retrieving the molecular structure from the diffraction data in Fig. 2. One data set corresponds to perfect 1D alignment [Fig. 2(a)], the other to a realistically achievable degree of alignment [Fig. 2(b)]. The $Q_\parallel$-$Q_\perp$ coverage in Fig. 2 suggests a real-space resolution slightly better than 1 Å. However, a comparison between panels (a) and (b) in Fig. 2 indicates that the effective resolution available in the case of imperfect alignment is only about 3 Å. In each dimension, the reciprocal space resolution was chosen to be 0.287 $Å^{-1}$, which gives an oversampling rate of twice the Nyquist rate.[11]

Assuming perfect 1D alignment, the cylindrically averaged scattering intensity may be approximated by[25]

$$I(Q_\perp,Q_\parallel)=\sum_m |A_m(Q_\perp,Q_\parallel)|^2, \tag{2}$$

where

$$A_m(Q_\perp,Q_\parallel)=\sum_j f_j e^{iQ_\parallel z_j} i^m J_m(Q_\perp r_j) \tag{3}$$

represents the mth cylindrical harmonic of the scattered amplitude. The sum in Eq. (3) is over the atoms constituting the molecule, f_j is the form factor of atom j, z_j and r_j are real-space cylindrical coordinates of atom j with respect to the alignment axis, and J_m is a Bessel function of mth order. The summation in Eq. (2) is often a highly truncated series. In particular, for a small molecule with an n-fold rotation axis of sufficiently high n, Eq. (2) may be well approximated by just the $m=0$ term.[25] An explicit calculation showed this to be the case here ($n=3$). Since this condition holds, one can attempt to reconstruct the azimuthal projection of CF_3Br using the phase-retrieval algorithm described in Ref. 25.

The algorithm begins by approximating $|A_0(Q_\perp,Q_\parallel)|$ by $\sqrt{I(Q_\perp,Q_\parallel)}$, initially assigning random phases to the amplitudes, and finding a first estimate of the azimuthally projected electron density $\rho_0(r,z)$ of the molecule via a Fourier–Hankel transform. (The intensities in the missing wedges are initially set to zero.) A suitable object-domain operation[30] is now applied to $\rho_0(r,z)$ and a new estimate of $A_0(Q_\perp,Q_\parallel)$ is found by an inverse Fourier–Hankel transform. The phases of $A_0(Q_\perp,Q_\parallel)$ are retained, but, where available, their absolute values are again constrained to $\sqrt{I(Q_\perp,Q_\parallel)}$. In the missing wedges, both the phases *and* amplitudes are retained. The cycle of iterations between reciprocal and real space is repeated until convergence. The effectiveness of such an algorithm in reconstructing the azimuthal projection of a short segment of a single-wall carbon nanotube to about 3 Å resolution has been demonstrated.[25] However, when we applied the above algorithm to the patterns in Fig. 2, we obtained variable results depending on the choice of initial random phases at the start of the iterations.

An alternative approach to reconstructing an azimuthal projection of the molecule is to exploit a special feature of CF_3Br, which lends itself to a solution similar to the "heavy atom" method of x-ray crystallography.[31] Another way to understand the following algorithm is by analogy to holography.[32] A hologram may be thought of as a diffraction pattern consisting of the square modulus of a superposition of a relatively large *reference wave* of known form and an unknown *object wave*. In this case, the scattering intensities become linear in the unknown object wave and its conjugate, thus allowing the reconstruction of the object giving rise to the object wave. X-ray holography is discussed, for instance, in Refs. 33 and 34.

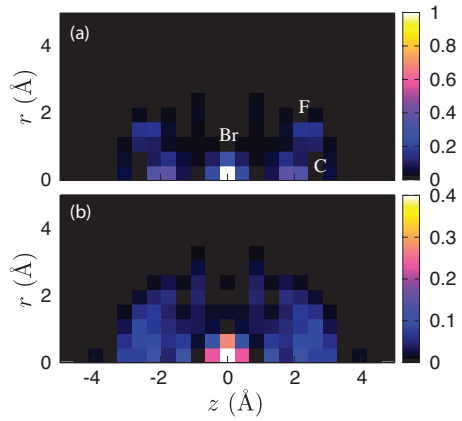

FIG. 3. The azimuthally projected structure $\tilde{\rho}_0(r,z)$ of CF_3Br, holographically reconstructed from the simulated diffraction patterns of Fig. 2. (a) Perfect 1D alignment and (b) laser-induced alignment.

Here, the form factor of one of the atoms of the molecule, Br ($Z=35$), dominates over those of F ($Z=9$) and C ($Z=6$). The right-hand side of Eq. (2) may therefore be further approximated by

$$I(Q_\perp,Q_\parallel)\simeq |A_0(Q_\perp,Q_\parallel)|^2 \simeq |f_0|^2+\left\{\sum_{j\neq 0} f_0^* f_j e^{iQ_\parallel z_j} J_0(Q_\perp r_j)+\text{c.c.}\right\}, \tag{4}$$

where c.c. denotes the complex conjugate. In Eq. (4), the real-space coordinate system was chosen such that the Br atom ($j=0$) is located at the origin ($r_0=z_0=0$). If the reconstruction algorithm

$$\tilde{\rho}_0(r,z)=\int Q_\perp I(Q_\perp,Q_\parallel)e^{-iQ_\parallel z}J_0(Q_\perp r)dQ_\perp dQ_\parallel \tag{5}$$

is applied to $I(Q_\perp,Q_\parallel)$, it may be seen, by substituting Eq. (4) into Eq. (5), that

$$\frac{r\tilde{\rho}_0(r,z)}{2\pi}\simeq |f_0|^2\delta(z)\delta(r)+\sum_{j\neq 0}\delta(r-r_j) \times\{f_0^* f_j\delta(z-z_j)+f_0 f_j^*\delta(z+z_j)\}, \tag{6}$$

assuming relatively slow variations of f_j with $Q_\perp$ and $Q_\parallel$. That is, one would expect the reconstruction $\tilde{\rho}_0(r,z)$ to show peaks at the cylindrical coordinates r_j, z_j of the atoms of the molecule, with some enhancement of intensity close to the cylinder axis. In addition, a twin image[32] with peaks at r_j, $-z_j$ is obtained. Note that Eq. (5) defines a single-pass, noniterative algorithm, which does not depend on an initial choice of random phases, and, as such, produces a unique result for a particular diffraction pattern.

Figure 3 shows the molecular structures reconstructed, using Eq. (5), from the diffraction patterns in Fig. 2. In order to prevent the overshadowing of the C and F atoms by the Br atom, the intensities of a 3×6 array of central pixels have been artificially reduced by a factor of 5. All pixels with

negative intensity have been set to zero. In the case of perfect 1D alignment [Fig. 3(a)], the atomic constituents of CF_3Br (and its holographic twin image) are clearly visible. However, considerable smearing of the C and F atoms is seen in the reconstruction from laser-aligned CF_3Br [Fig. 3(b)]. The smearing is consistent with the imperfect alignment achieved under the conditions considered. At $\langle \cos^2 \theta_{ml} \rangle = 0.87$, the C atom, for instance, is expected to be displaced from the alignment axis by, on average, two pixels.

The unphysical electron density near $r=2$, $z=\pm 1$ in Fig. 3 is a consequence of the missing wedges. Its presence is not apparent in panel (a) because the density of the sharper F atoms in Fig. 3(a) is about twice as large as that of the smeared-out F electron cloud in Fig. 3(b). Since Eq. (5) defines a noniterative procedure, it is not possible to recover the scattering information in the missing wedges.

In conclusion, we investigated the capabilities of algorithms for reconstructing the electron density of a symmetric-top molecule aligned by a high-intensity laser. The reconstructed electron density is unavoidably azimuthally averaged. We find that an iterative phasing algorithm[25] does not yield sufficiently reproducible results. This could be due to the heavy Br dominating the scattering, and/or because one is operating at the resolution limit of the x-ray scattering arrangement. However, reliable reconstruction was achieved using an algorithm inspired by holographic concepts. We find that even a laser intensity as high as 1.9×10^{12} W/cm^2 does not provide sufficient molecular alignment for atomic-resolution imaging of small molecules such as CF_3Br. A higher laser intensity might make it possible to confine the rotational motion more strongly, but would most likely lead to laser-induced structural distortion.

We thank Henry Chapman for an inspiring discussion. We acknowledge support from the Office of Basic Energy Sciences, Office of Science, U.S. Department of Energy as follows: Contract No. DE-AC02- 06CH11357 (P.J.H. and R.S.), Grant Nos. DE-FG02-84ER45076 and DE-FG02-06ER46277 (V.L.S. and D.K.S.), and Grant No. DE- FG03-02ER45996 (D.S.).

[1] K. Yamanouchi, Science **295**, 1659 (2002).
[2] C. Wunderlich, E. Kobler, H. Figger, and T. W. Hänsch, Phys. Rev. Lett. **78**, 2333 (1997).
[3] B. J. Sussman, D. Townsend, M. Yu. Ivanov, and A. Stolow, Science **314**, 278 (2006).
[4] E. Constant, H. Stapelfeldt, and P. B. Corkum, Phys. Rev. Lett. **76**, 4140 (1996).
[5] T. Seideman, M. Yu. Ivanov, and P. B. Corkum, Phys. Rev. Lett. **75**, 2819 (1995).
[6] A. Iwasaki, A. Hishikawa, and K. Yamanouchi, Chem. Phys. Lett. **346**, 379 (2001).
[7] M. Comstock, V. Senekerimyan, and M. Dantus, J. Phys. Chem. A **107**, 8271 (2003).
[8] J. H. Posthumus, Rep. Prog. Phys. **67**, 623 (2004).
[9] V. G. Stavros, E. Harel, and S. R. Leone, J. Chem. Phys. **122**, 064301 (2005).
[10] K. J. Gaffney and H. N. Chapman, Science **316**, 1444 (2007).
[11] J. Miao, T. Ishikawa, Q. Shen, and T. Earnest, Annu. Rev. Phys. Chem. **59**, 387 (2008).
[12] J. C. H. Spence and R. B. Doak, Phys. Rev. Lett. **92**, 198102 (2004).
[13] J. C. H. Spence, K. Schmidt, J. S. Wu, G. Hembree, U. Weierstall, B. Doak, and P. Fromme, Acta Crystallogr., Sect. A: Found. Crystallogr. **61**, 237 (2005).
[14] D. Starodub, R. B. Doak, K. Schmidt, U. Weierstall, J. S. Wu, and J. C. H. Spence, J. Chem. Phys. **123**, 244304 (2005).
[15] E. R. Peterson, C. Buth, D. A. Arms, R. W. Dunford, E. P. Kanter, B. Krässig, E. C. Landahl, S. T. Pratt, R. Santra, S. H. Southworth, and L. Young, Appl. Phys. Lett. **92**, 094106 (2008).
[16] H. Stapelfeldt and T. Seideman, Rev. Mod. Phys. **75**, 543 (2003).
[17] J. J. Larsen, K. Hald, N. Bjerre, H. Stapelfeldt, and T. Seideman, Phys. Rev. Lett. **85**, 2470 (2000).
[18] J. G. Underwood, B. J. Sussman, and A. Stolow, Phys. Rev. Lett. **94**, 143002 (2005).
[19] K. F. Lee, D. M. Villeneuve, P. B. Corkum, A. Stolow, and J. G. Underwood, Phys. Rev. Lett. **97**, 173001 (2006).
[20] B. Friedrich and D. Herschbach, J. Chem. Phys. **111**, 6157 (1999).
[21] R. Baumfalk, N. H. Nahler, and U. Buck, J. Chem. Phys. **114**, 4755 (2001).
[22] S. Minemoto, H. Nanjo, H. Tanji, T. Suzuki, and H. Sakai, J. Chem. Phys. **118**, 4052 (2003).
[23] L. Holmegaard, J. H. Nielsen, I. Nevo, H. Stapelfeldt, F. Filsinger, J. Küpper, and G. Meijer, Phys. Rev. Lett. **102**, 023001 (2009).
[24] V. Elser and R. P. Milane, Acta Crystallogr., Sect. A: Found. Crystallogr. **64**, 273 (2008).
[25] D. K. Saldin, V. L. Shneerson, D. Starodub, and J. C. H. Spence, "Reconstruction from a single diffraction pattern of azimuthally projected electron density of molecules aligned parallel to a single axis," Acta Crystallogr. A (to be published).
[26] C. Buth and R. Santra, J. Chem. Phys. **129**, 134312 (2008).
[27] P. J. Ho and R. Santra, Phys. Rev. A **78**, 053409 (2008).
[28] U. Even, J. Jortner, D. Noy, and N. Lavie, J. Chem. Phys. **112**, 8068 (2000).
[29] R. Fung, V. L. Shneerson, D. K. Saldin, and A. Ourmazd, Nat. Phys. **5**, 64 (2009).
[30] J. R. Fienup, Appl. Opt. **21**, 2758 (1982).
[31] W. L. Bragg, Nature (London) **143**, 678 (1939).
[32] D. Gabor, Nature (London) **161**, 777 (1948).
[33] C. S. Fadley and P. M. Len, Nature (London) **380**, 27 (1996).
[34] L.-M. Stadler, C. Gutt, T. Autenrieth, O. Leupold, S. Rehbein, Y. Chushkin, and G. Grübel, Phys. Rev. Lett. **100**, 245503 (2008).